NACA

RESEARCH MEMORANDUM

FLIGHT CALIBRATION OF FOUR AIRSPEED SYSTEMS ON A

SWEPT-WING AIRPLANE AT MACH NUMBERS UP TO 1.04

BY THE NACA RADAR-PHOTOTHEODOLITE METHOD

By Jim Rogers Thompson, Richard S. Bray,
and George E. Cooper

Ames Aeronautical Laboratory
Moffett Field, Calif.

ENGINEERING DEPT. LIBRARY
CHANCE-VOUGHT AIRCRAFT
DALLAS, TEXAS

NATIONAL ADVISORY COMMITTEE
FOR AERONAUTICS

WASHINGTON
October 27, 1950

NATIONAL ADVISORY COMMITTEE FOR AERONAUTICS

RESEARCH MEMORANDUM

FLIGHT CALIBRATION OF FOUR AIRSPEED SYSTEMS ON A SWEPT-WING

AIRPLANE AT MACH NUMBERS UP TO 1.04 BY THE NACA

RADAR-PHOTOTHEODOLITE METHOD

By Jim Rogers Thompson, Richard S. Bray, and
George E. Cooper

SUMMARY

The calibrations of four airspeed systems installed in a North American F-86A airplane have been determined in flight at Mach numbers up to 1.04 by the NACA radar-phototheodolite method. The variation of the static-pressure error per unit indicated impact pressure is presented for three systems typical of those currently in use in flight research, a nose boom and two different wing-tip booms, and for the standard service system installed in the airplane. A limited amount of information on the effect of airplane normal-force coefficient on the static-pressure error is included. The results are compared with available theory and with results from wind-tunnel tests of the airspeed heads alone.

Of the systems investigated, a nose-boom installation was found to be most suitable for research use at transonic and low supersonic speeds because it provided the greatest sensitivity of the indicated Mach number to a unit change in true Mach number at very high subsonic speeds, and because it was least sensitive to changes in airplane normal-force coefficient. The static-pressure error of the nose-boom system was small and constant above a Mach number of 1.03 after passage of the fuselage bow shock wave over the airspeed head.

INTRODUCTION

Accurate determination of Mach number is fundamental to any detailed flight research, and is of particular importance in the transonic speed range where many of the aerodynamic parameters vary markedly with Mach number. In order to pursue extensive research in this speed range, using a North American F-86A airplane as a test vehicle, it was necessary that a suitable airspeed system be determined. In addition, it was desired

to supplement the meager fund of information now available to the designer
on the characteristics of various airspeed installations at transonic
speeds.

　　　With the foregoing objectives in mind, four independent airspeed
systems, one service and three research installations typical of those
used at high subsonic speeds, were evaluated at Mach numbers up to 1.04
by the NACA radar–phototheodolite method of reference 1. The results
have been supplemented with data from calibrations at Mach numbers up to
0.89 obtained by flying past a reference landmark. This technique is
described in reference 2. Also presented are the results of wind–tunnel
tests of the airspeed heads used in the research installations. These
tests were conducted in the Ames 16–foot high–speed wind tunnel and the
Ames 6– by 6–foot supersonic wind tunnel.

　　　The radar–phototheodolite calibrations were performed jointly by
personnel of the Ames Aeronautical Laboratory and the High–Speed Flight
Research Station of the NACA.

SYMBOLS

A_Z　　the ratio of the net aerodynamic force along the airplane Z axis
　　　　(positive when directed upward, as in normal level flight) to the
　　　　weight of the airplane

C_N　　airplane normal–force coefficient $\left(\dfrac{W A_Z}{q S}\right)$

M　　　Mach number

M'　　indicated Mach number

R　　　gas constant, 1716 foot–pounds per pound per $^{\circ}R$

S　　　wing area, square feet

T　　　ambient temperature, $^{\circ}R$

V　　　airspeed, feet per second

W　　　weight of airplane, pounds

g　　　acceleration due to gravity, 32.2 feet per second squared

h　　　geometric altitude from sea level, yards

p　　　free–stream static pressure, millimeters of mercury

p'   static pressure indicated by pitot-static installation, millimeters
       of mercury

Δp static-pressure error $(p'-p)$, millimeters of mercury

p_s static pressure corresponding to NACA standard atmosphere, millimeters
       of mercury

p_t free-stream total pressure for subsonic flow and total pressure behind
       normal shock for supersonic flow, millimeters of mercury

q   dynamic pressure $\left(\frac{1}{2} \rho V^2 \right)$, pounds per square foot

q_c' indicated impact pressure (p_t-p'), millimeters of mercury

ρ density of air, slugs per cubic foot

λ_o lag constant, seconds

EQUIPMENT

Airspeed Systems

The airplane used in the investigation (North American F-86A-5 Air
Force No. 48-291) was equipped with three research airspeed installations,
a nose boom and two wing-tip booms, in addition to the standard service
system. Kollsman Type D-1 (BuAer Spec. No. SQ-107) airspeed heads were
mounted on the nose and left wing-tip booms and an NACA free-swiveling
airspeed head was mounted on the right wing-tip boom. Pertinent dimensions
of the test airplane are presented in table I and a two-view drawing of the
airplane showing all four airspeed systems is presented as figure 1. Photo-
graphs of the installations are presented as figure 2 and drawings of the
heads are presented in figure 3.

In order to minimize the effects of the pressure field about the air-
plane upon the static-pressure measurements, the static orifices of the
research airspeed installations were located well forward of the airplane
structure. The static orifices of the nose-boom installation were located
ahead of the airplane nose a distance of 1.8 times the effective maximum
diameter of the fuselage. (This diameter is defined as that of a circle
having the same area as the fuselage cross section, including the area of
the duct.) On the left and right wing-tip booms the static orifices were
located 1.5 tip-chord lengths and 1.1 tip-chord lengths ahead of the
respective leading edges. The two flush static orifices of the service
airspeed system were located on opposite sides of the lower quadrant of

the fuselage ahead of the wing root. (See fig. 1.) Total pressure for
the service system was supplied by a total-head tube located in the engine
air inlet. Since the impact pressure (and therefore the total head) was
not measured for the swiveling airspeed head, total-head measurements
from the nose-boom system were used to determine the calibration of this
system.

Flight Instruments

Standard two-cell NACA pressure recorders were used to measure the
pressures in each of the airspeed systems. The absolute static pressure
in each system was measured by a sensitive aneroid cell, and the difference
between static pressure and total head (the impact pressure q_c') was meas-
ured by a differential pressure cell. In addition to the pressure recorders,
a normal acceleration recorder was provided so that the airplane normal-
force coefficient could be derived. The recording instruments were syn-
chronized at 1/10-second intervals by means of a common timing circuit.

For the research airspeed systems, the pressure orifices were connected
to the individual cells through 3/16-inch internal diameter lines about 12
feet long in the case of the nose boom, and about 30 feet long in the case
of the wing booms. The lag in the static side of the system was measured
for the left-wing-boom system by the method of reference 2, and the equiv-
alent sea-level time lag (λ_0) was found to be of the order of 0.03 second.
The lag of the right-wing-boom system may be presumed to be of the same
order, as the lines are of almost identical length, and that of the nose
boom may be presumed to be smaller than that of the wing boom. The service
system supplies the pilot's indicators as well as the recorder, and the
volume of these instruments is many times greater than that of the research
instruments. However, the lines of the service system are very short. The
lag for a similar system is computed in reference 2 to be of the order of
0.02 second. No corrections for lag were applied.

Free-air temperature was obtained in flight using the service instal-
lation which employed a Weston Type 21 flush-type resistance bulb located
near the starboard static orifice of the service airspeed system. Data
were noted by the pilot. The adiabatic constant of the system was deter-
mined by flight measurements through a wide range of Mach numbers.

Tracking Station

The ground tracking station was equipped with an SCR-584 radar modified
for long-range operation, an M-2 optical tracking head, a German Askania
phototheodolite, and a VHF radio communication system. In operation, the
airplane was tracked optically by both the Askania and the M-2, the M-2
pointing the radar unit at the airplane through a servo system. The data

were recorded at the ground station by two cameras which were operated
at a rate of two exposures per second. One of the cameras, an integral
part of the Askania phototheodolite, photographed direct reading scales
giving the azimuth and elevation angles. This camera also photographed
the airplane against reference cross hairs to provide corrections to the
azimuth and elevation angles in the cases where the airplane was not
centered in the cross hairs. The other camera photographed the radar
range scope giving the distance from the radar station to the airplane.
The time at which each frame of each camera was taken and the flight-
instrument synchronization signals transmitted by radio from the airplane
were recorded against a continuous time base. The airplane was equipped
with radar beacons on both the upper and lower surface of the fuselage
so that the usable range of the radar could be extended.

METHOD

In accordance with normal practice, it was assumed that no error
existed in the indicated total pressure (obtained by adding indicated
static and impact pressures) through the range of Mach numbers and flow
angles encountered in this investigation. The calibration was, therefore,
limited to determining the error in the indicated static pressure. The
flight technique used was essentially the same as that described in ref-
erence 1. The service system, nose-boom, and left-wing-boom systems were
first calibrated from 0.30 to 0.89 Mach number at sea level by the method
described in reference 2 of flying past a reference landmark (referred
to hereafter as the "fly-by" calibration).

The variation of ambient pressure with geometric altitude in the
altitude range to be covered by the high-speed runs was established by a
pressure survey. Static-pressure records were taken at altitude inter-
vals of about 1,000 feet during the climb of the test airplane at speeds
within the range covered by the fly-by calibration. By use of a time
synchronization system, static pressures were determined at time instants
corresponding to those of two Askania frames from each record. The Mach
number and the static pressure were computed from the airplane records
through use of the fly-by calibration. The corresponding geometric
altitude was computed from the basic quantities measured at the ground
station with corrections being applied for the following items:

1. Elevation angle scale zero, level error, tracking error, and
   refraction correction

2. Range scale zero, beacon delay, and range parallax (due to
   horizontal distance between radar and Askania)

3. Earth curvature correction

Values of ambient pressure obtained from the nose- and wing-boom systems were plotted against the corresponding geometric altitude determined by the foregoing procedure. An additional guide to the fairing of these data was obtained from the known relation of incremental altitude to incremental pressure when the temperature and pressure are known. Temperature data were obtained at each survey point. An altitude-pressure relationship was then computed from the basic relation

$$\frac{dh}{dp} = -\frac{R}{g}\frac{T}{p}.$$

using the approximate form

$$h_2 - h_1 = K\left(\frac{T}{p}\right)(p_1 - p_2)$$

where $H_2 - h_1$ is the change in altitude corresponding to a pressure change $p_1 - p_2$, and K is a constant depending on the units of the various quantities. Pressure increments of 20 millimeters of mercury were used in these computations. The resulting altitude-pressure curve was then compared with that determined by the pressure survey. A typical survey obtained with the nose-boom system and the associated temperature fairing is shown in figure 4 as the variation with geometric altitude of the difference between ambient pressure as determined in the survey and ambient pressure at the same altitude for standard conditions.

During the high-speed runs, the geometric altitude was determined at 1-second intervals by the same procedure used for the survey. The ambient pressures corresponding to these altitudes were obtained from the results of the pressure survey made during the climb. A time history of ambient pressure was then compared with time histories of the static pressure indicated by each of the airspeed systems. The pressure error was determined for each system from the time history and reduced to nondimensional form by division by the indicated impact pressure $q_c{}'$. True and indicated Mach numbers were computed from total pressure and the appropriate value of static pressure.

ACCURACY

Flight Measurements

The maximum probable uncertainty in pressure measurements is estimated to be of the order of ± 2 millimeters of mercury under the conditions of altitude and temperature experienced in this investigation.

Values of free-air temperature obtained from the indicating system in the airplane are estimated to have been determined with a precision of $\pm 5^{\circ}$ F.

Geometric Altitude Measurements

The basic quantities entering into the computation of the geometric altitude are the range and elevation angles. In this investigation, data were obtained at elevation angles between 15° and 55° and ranges between 14,000 and 38,000 yards, although the great majority of the data were obtained at ranges between 20,000 and 25,000 yards at elevation angles near 30°. Examination of time histories of the indicated radar range for each run indicated that the maximum scatter of over 90 percent of the points from a smooth fairing was about ± 15 yards which corresponds to a precision in measurement of geometric altitude of ± 4 yards and ± 12 yards, respectively, for the extremes of elevation angle encountered. The probable uncertainty in an elevation angle measured with an Askania phototheodolite is given by reference 3 as ± 1 minute, which, for the extreme conditions encountered, amounts to from 3 to 10 yards in geometric altitude. It is therefore estimated that the probable uncertainty in geometric altitude during the high-speed test runs is of the order of ± 10 yards. This value of altitude uncertainty corresponds to pressure uncertainties of ± 0.25 and ± 0.16 mm Hg at altitudes of 35,000 and 45,000 feet, respectively. It is apparent that the resulting uncertainty in true static pressure from the geometric altitude measurements is considerably less than that due to the pressure instruments.

Summary of Accuracy

Since the errors in measurement enter into both the pressure survey and the actual calibration flight, the individual errors must be added to establish the maximum possible error in the final result. This would give a value for the uncertainty in Δp of ± 4.5 mm Hg. It is reasonable to assume, however, that the probable uncertainty in Δp is of the order of ± 2 mm Hg. The following table summarizes the resultant uncertainties in $\Delta p/q_c'$ and Mach number at the conditions of the radar-phototheodolite calibration:

Mach number, M	0.75	0.85	0.95	1.04
Average impact pressure, q_c', mm Hg	60	100	160	180
Probable uncertainty in $\Delta p/q_c'$	± 0.03	± 0.02	± 0.01	± 0.01
Probable uncertainty in M	± 0.015	± 0.012	± 0.009	± 0.009

RESULTS

Typical time histories of Mach number M, airplane normal-force coefficient C_N, ambient pressure p, indicated static pressure p' for each system, and static-pressure error per unit indicated impact pressure $\Delta p/q_c'$ for each system are presented in figure 5 for both a high-speed run (fig. 5(a)) and a pull-up (fig. 5(b)). These time histories illustrate the magnitude of the pressure errors as well as the variation of pertinent quantities during transition through the speed of sound and during an abrupt pull-up.

The results obtained for each system are summarized in figure 6 as the variation with Mach number of $\Delta p/q_c'$. Where available, fly-by data are used up to a Mach number of 0.89 because of the reduced accuracy of the radar-calibration data at lower Mach numbers. Since the right-wing-boom system was not included in the fly-by calibrations, radar-calibration data are shown for the lower Mach numbers (fig. 6(d)). Figure 7 presents the variation with normal-force coefficient of $\Delta p/q_c'$ for several ranges of Mach number. It is evident from examination of figure 6 that the apparently random scatter of the experimental data is the same order as estimated in the section ACCURACY.

DISCUSSION

Nose Boom

The experimental data obtained with the nose-boom airspeed system using a fixed pitot-static head (fig. 2(b)) are presented in figures 6(a) and 7(a).

Effects of Mach number.- The results shown in figure 6(a) indicate that the value of $\Delta p/q_c'$ remains constant at a value of 0.025 up to a Mach number of 0.95. As shown in the figure, this value is in agreement with that obtained in the sea-level fly-by calibration, which extends to a Mach number of 0.89. Above a Mach number of 0.95 the error increases almost linearly to 0.065 at a Mach number of 1.02. This rapid increase is apparently due to the effect of compressibility upon the static pressure field ahead of the fuselage. Between Mach numbers 1.02 and 1.04 the value of $\Delta p/q_c'$ is -0.008. The abrupt decrease in error which occurs with passage of the fuselage bow wave over the static orifices on the airspeed head is illustrated by a typical instrument record in figure 8, as well as the corresponding time history in figure 5(a). In this case the abrupt drop occurred at a Mach number of 1.028, and the bow wave remained behind the orifices for about 10 seconds, passing the orifices in the opposite direction when the Mach number fell off to 1.015. In the other run in which a speed high enough for the bow wave to pass the orifices

was attained, the passage occurred at a Mach number of 1.021 and the return again occurred at a Mach number of 1.015. Although the Mach numbers quoted for the initial and return shock passage differ by an amount within the limits of accuracy of Mach number determination and are therefore not necessarily significant, the possible existence of a hysteresis effect should not be ignored in future research. It is of interest to note in figure 8 that the response of the instrument recording static pressure to passage of the shock over the static orifices corresponds in shape to the expected response to a step change in pressure. The change of 0.075 in $\Delta p/q_c'$ with shock passage is in satisfactory agreement with the theoretical pressure drop of 0.066 across a normal shock wave at a Mach number of 1.025.

The fairing of the data given in figure 6(a) is reproduced in figure 9 where it is compared with wind-tunnel measurements of the static-pressure error of Kollsman D-1 type airspeed heads. The wind-tunnel data for Mach numbers below 0.85 were obtained in the Ames 16-foot high-speed tunnel and show a constant static-pressure error for the airspeed head alone of about 0.006 $\Delta p/q_c'$. The difference of approximately 0.02 $\Delta p/q_c'$ between the experimental values for the error of the nose-boom system on the airplane and the error of the head alone may be considered to be a measure of the subsonic static-pressure field of the airplane at the nose-boom orifices. This compares favorably with theory as presented in figure 10(a) of reference 4. For this comparison, the 10-foot nose boom was considered to be mounted on a body of revolution having a maximum diameter of 5.5 feet at a distance of 9 feet aft of the nose of the body. An extrapolation of the curve in reference 4 gives a value of about 0.02 for $\Delta p/q_c'$.

The Ames 6- by 6-foot supersonic wind-tunnel data indicate that $\Delta p/q_c'$ for the isolated head and boom varies from 0.004 at a Mach number of 1.13 to 0.0005 at a Mach number of 1.60. If it is assumed that flight data would continue to show a value of $\Delta p/q_c'$ of -0.007 at Mach numbers above 1.04, the agreement with the wind-tunnel data at a Mach number of 1.13 would be within the accuracy of the measurements.

Effects of normal-force coefficient.- It is evident from figure 7(a) that the effect of airplane normal-force coefficient on $\Delta p/q_c'$ for the nose-boom system is negligible for the range of variables investigated: airplane normal-force coefficients from 0.05 to 0.80 at Mach numbers between 0.75 and 0.95 and from 0.06 to 0.27 at Mach numbers between 0.95 and 1.04. This lack of effect is evident also in the time history of an abrupt pull-up (fig. 5(b)).

Left-Wing-Boom System

Results for the airspeed system consisting of a fixed head mounted 1.5 tip-chord lengths ahead of the left wing tip are shown in figures 6(b) and 7(b).

Effects of Mach number.– Figure 6(b) reveals that $\Delta p/q_c{}'$ decreases steadily from about 0.004 at a Mach number of 0.75 to –0.007 at a Mach number of 0.91. As the subsonic wind–tunnel data for the airspeed head, presented in figure 9, show a small, constant, positive error at these speeds, the decrease is presumed to be due to the change in the pressure field of the wing accompanying the changes in speed and lift coefficient. Above a Mach number of 0.91, $\Delta p/q_c{}'$ increases at an increasing rate, reaching a value of about 0.06 near a Mach number of 1.02 and then decreases rapidly to 0.03 near M=1.04, the highest test Mach number. It should be noted that the increase in error which occurs as the speed of sound is approached amounts to about 0.07 $\Delta p/q_c{}'$ for a Mach number change from 0.91 to 1.02. This change is about twice that shown to occur for the nose–boom system in figure 6(a).

Effects of normal–force coefficient.– From figure 7(b) it is apparent that, for Mach numbers between 0.75 and 0.95, $\Delta p/q_c{}'$ increases with an increase in airplane normal–force coefficient, a change in normal–force coefficient from 0.10 to 0.70 causing an increase in $\Delta p/q_c{}'$ of about 0.04. The data presented are considered inadequate to show a consistent effect of normal–force coefficient at Mach numbers greater than 0.95.

Right–Wing–Boom System

The third research–type system consisted of an NACA full–swiveling airspeed head mounted on a boom 1.1 tip–chord lengths ahead of the right wing tip. Results of a calibration of this installation are shown in figures 6(c) and 7(c).

Effects of Mach number.– Figure 6(c) shows that $\Delta p/q_c{}'$ remains at a relatively small positive value up to a Mach number of 0.90, increases rapidly from about 0.023 to over 0.12 near a Mach number of 1.02, and then decreases to about 0.10 at a Mach number of 1.04. The variation of $\Delta p/q_c{}'$ with Mach number measured for the right–wing–boom system is similar to that measured for the left–wing–boom system, the only significant differences being the level at subsonic speeds and the more rapid increase in error as the speed of sound is approached for the right–wing–boom system. The different level at subsonic speeds results from the relatively large effect of the NACA swiveling airspeed head on the local static-pressure field. The large increase in $\Delta p/q_c{}'$ as the speed of sound is approached probably results both from the larger effect of the head and the increase in the effect of the wing due to the shorter boom length, one tip chord compared to one and one–half tip chords.

The results for the right–wing–boom system are compared with the wind–tunnel data for the swiveling airspeed head in figure 10. The subsonic results from the Ames 16–foot high–speed wind tunnel show that $\Delta p/q_c{}'$ for the isolated airspeed head is about 0.01 at a Mach number of 0.3 and increases to about 0.02 at a Mach number of 0.85.

The Ames 6- by 6-foot supersonic wind-tunnel tests indicate an almost constant error for the boom and airspeed head of -0.010 $\Delta p/q_c'$ from 1.20 to 1.60 Mach number. No supersonic flight-test data comparable to that obtained on the nose boom are available since this head was evidently situated within the field of influence of the airplane shock waves.

Effects of normal-force coefficient.- The effects of the airplane normal-force coefficient on $\Delta p/q_c'$ for the right-wing-boom system are shown for Mach numbers between 0.75 and 1.05 in figure 7(c). No effect is apparent at normal-force coefficients below 0.55; above this value a slight increase in $\Delta p/q_c'$ with increasing normal-force coefficient is indicated. Since the maximum angle of free travel of the swiveling head was about ±30°, this result was evidently not an effect of inclination of the head. The data presented are again considered inadequate to determine the effect of changes in normal force on $\Delta p/q_c'$ at Mach numbers above 0.90.

Service Airspeed System

The service system employed a total-head tube located in the nose inlet and flush static-pressure orifices on either side of the lower fuse-lage forward of the wing root.

Effects of Mach number.- Data for this system as shown in figure 6(d) indicate that $\Delta p/q_c'$ is negative throughout the Mach number range. An abrupt change in the error from a value of -0.015 to -0.06 appears near a Mach number of 0.98. It is evident that this sudden change is not sim-ilar to that found on the nose boom. Recorded pressures in this speed range were erratic, and showed no well-defined discontinuity such as was seen with the nose-boom system (fig. 5). It is surmised that a bow wave of the wing root exists in the local supersonic flow field of the body, and that passage of this shock wave over the static orifices is responsible for the erratic nature of the recorded pressures. Asymmetry of the bow waves on each side due to variation of yaw angle might result in the mul-tiplicity of values obtained in this region.

Effects of normal-force coefficient.- It is evident from figure 7(d) that large changes in static-pressure error accompany increases in normal-force coefficient from 0.30 to 0.70. As a result, the indication of a Mach meter connected to the service system would change from about 0.93 to about 0.85 during a pull-up at a constant Mach number of 0.90. The data of figure 7(d) indicate that at Mach numbers above 0.95, large changes occur even within the small range of normal-force coefficients investi-gated. The difference in normal-force coefficients at which the fly-by and radar calibrations were made may account for the discrepancy between values of $\Delta p/q_c'$ at a Mach number of 0.89 as shown in figure 6(d).

Comparison of All Systems

The results of all four airspeed systems are compared in figure 11 which shows the variation of indicated Mach number with true Mach number. The results are also plotted in figure 12 as the variation with indicated Mach number of $\Delta p/q_c'$.

In flights subsequent to the radar—phototheodolite calibration, indicated Mach numbers as high as 1.09 have been recorded with the nose—boom airspeed system. From these flights, calibrations of the wing—tip systems between true Mach numbers of 1.04 and 1.08 were derived assuming that an extrapolation of the calibration of the nose—boom system remains constant at a $\Delta p/q_c'$ of −0.007. The resulting extrapolations of the calibration curves are included in figures 11 and 12.

These summary calibration curves illustrate one very undesirable result of the increases in static—pressure error at high subsonic speeds discussed previously. Particularly in the case of the right—wing boom it is seen that the increase in static—pressure error would reduce the response of the Mach number indicator to changes in true Mach number. This reduction in sensitivity may be sufficient to make the true Mach number indeterminate with the usual order of calibration accuracy. It is evident, therefore, that the usefulness and the accuracy of an airspeed system at transonic speeds are dependent upon the sensitivity of the indicated Mach number to a unit change in the true Mach number, that is, the slope dM'/dM.

Minimum values of the sensitivity are about 0.5 for the nose boom, 0.2 for both wing booms, and 0.4 for the service system. It is apparent from figure 11 that the region of reduced sensitivity is small for both the nose—boom and the left—wing—boom systems. However, the region of reduced sensitivity for the right—wing—boom system extends from 0.92 to 1.02 Mach number. The sensitivity of the service system does not reach low values where the calibration curve is well—defined; however, the presence of the region about a Mach number of 0.98 where the calibration is uncertain would make the system of doubtful value for some applications.

It is considered, therefore, that the nose—boom system would be the most suitable of the four systems investigated for use in flight research using this or a similar type airplane. In the present case, the uncertainty in determination of true Mach number between Mach numbers of 0.97 and 1.02 is twice that present at Mach numbers immediately above and below this range.

CONCLUSIONS

The calibrations of four independent airspeed systems installed in a North American F—86A—5 airplane have been determined in flight at Mach

numbers up to 1.04 by the NACA radar–phototheodolite method. In addition to the service installation, a nose–boom system and two wing–tip–boom systems were investigated. Evaluation of the results obtained and comparison with fly–by calibrations and wind–tunnel tests of the airspeed heads have led to the following conclusions:

1. The nose–boom system is considered to be the most suitable of the four systems investigated for the determination of Mach number in flight using this or similar airplanes because it provided the greatest sensitivity of the indicated Mach number to changes in true Mach number at high subsonic speeds, and because it was the least sensitive to airplane normal–force coefficient.

2. Minimum values of the sensitivity of each airspeed system, expressed as the change in indicated Mach number per unit change in true Mach number, were about 0.5 for the nose–boom systems, 0.2 for both wing–boom systems, and about 0.4 for the service airspeed system. A region was present in the service airspeed system about a Mach number of 0.98 where there appeared to be no consistent relation between the true Mach number and the indicated Mach number.

3. Changes in the airplane normal–force coefficient had no apparent effect on the nose–boom system and only minor effects on the wing–boom systems. The service airspeed system, however, showed a large increase in static–pressure error with increase in normal–force coefficient.

Ames Aeronautical Laboratory,
    National Advisory Committee for Aeronautics,
        Moffett Field, Calif.

<div align="center">REFERENCES</div>

1. Zalovcik, John A.: A Radar Method of Calibrating Airspeed Installations on Airplanes in Maneuvers at High Altitudes and at Transonic and Supersonic Speeds. NACA TN 1979, 1949.

2. Huston, Wilbur B.: Accuracy of Airspeed Measurements and Flight Calibration Procedures. NACA TN 1605, 1948.

3. Swanson, Margaret D.: Accuracy of NAMTC Phototheodolite System. Technical Memo Report No. 21, U. S. Naval Air Missile Test Center (Point Mugu), 1948.

4. Danforth, Edward C. B., and Johnston, J. Ford: Error in Airspeed Measurement Due to Static–Pressure Field Ahead of Sharp–Nose Bodies of Revolution at Transonic Speeds. NACA RM L9C25, 1949.

TABLE I.— PERTINENT DIMENSIONS OF TEST AIRPLANE

Wing

    Total wing area . . . . 287.9 sq ft
    Span . . . .   37.1 ft
    Aspect ratio. 4.79
    Taper ratio 0.51
    Mean aerodynamic chord . . . .   97.03 in.
    Dihedral angle. . . . .   3.0°
    Sweepback of 0.25—chord line. . . . .   35°14'
    Sweepback of leading edge . . . .   37°44'
    Aerodynamic and geometric twist (washout) . . . . . .   2.0°
    Root airfoil section (normal to 0.25—
      chord line) . . . . NACA 0012–64
                                                              (modified)
    Tip airfoil section (normal to 0.25—
      chord line) . . . . NACA 0011–64
                                                              (modified)
    Root chord (wing—fuselage intersection)   10.3 ft
    Tip chord . . . .   5.1 ft

Fuselage

    Length . . . .   34.0 ft
    Width (wing roots). . . . .   5.0 ft

Service airspeed system

    Static orifices (fuselage station 82,
      waterline —32.6)
        Distance ahead of wing leading edge
          at root . . . .   29.5 in.
        Distance below canopy base. . . . .   50.5 in.
    Total—head tube (inside duct at fuselage
      station 19.4)
        Distance of pressure source below
          upper duct surface. . . . .   2–15/16 in.
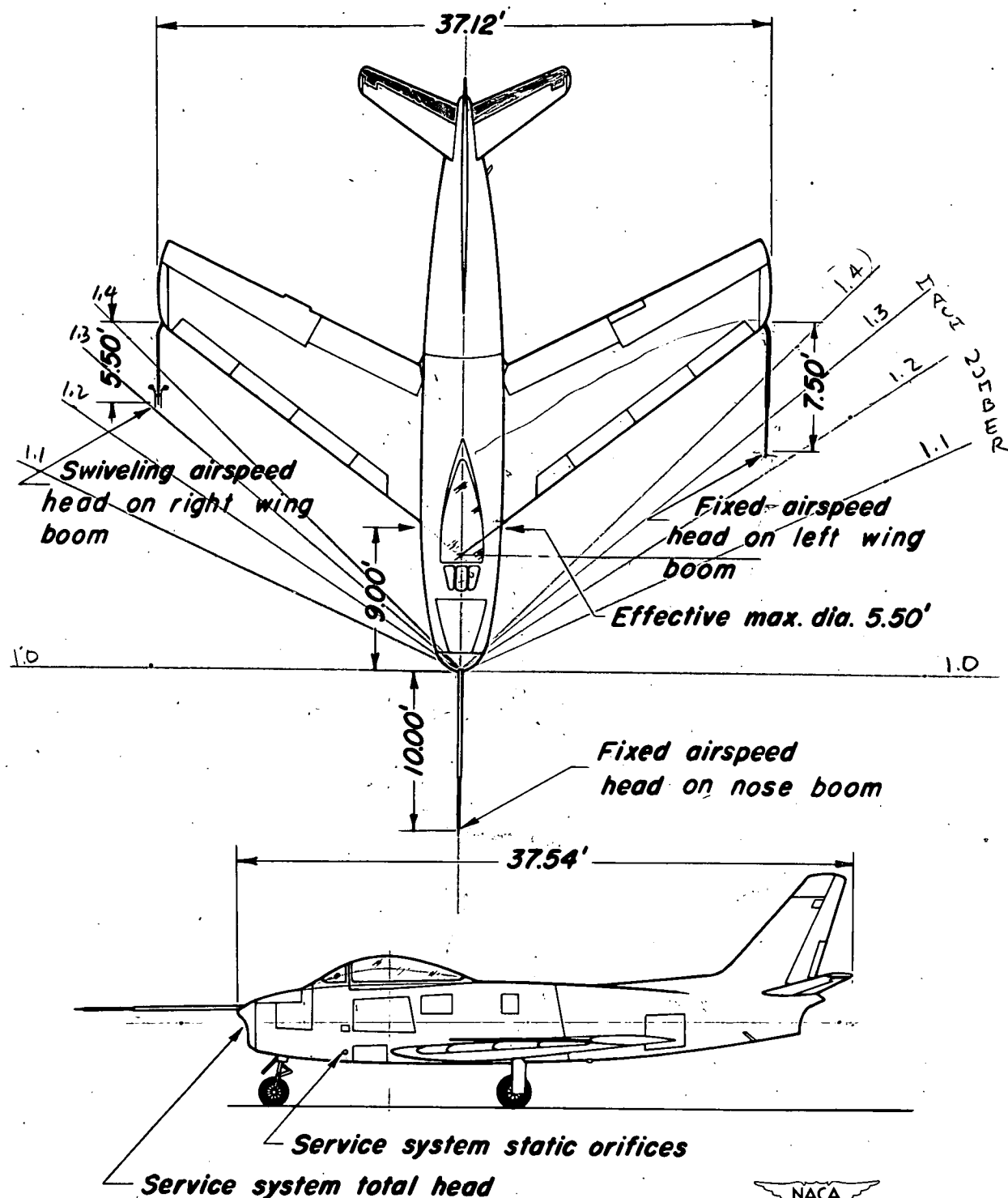
Figure 1.- Two-view drawing of test airplane showing airspeed installations.

Page intentionally left blank

Page intentionally left blank

(a) Complete airplane.

Figure 2.— Photographs of the airspeed systems on the test airplane.

Page intentionally left blank

(b) Nose boom.

Figure 2.— Continued.

Page intentionally left blank
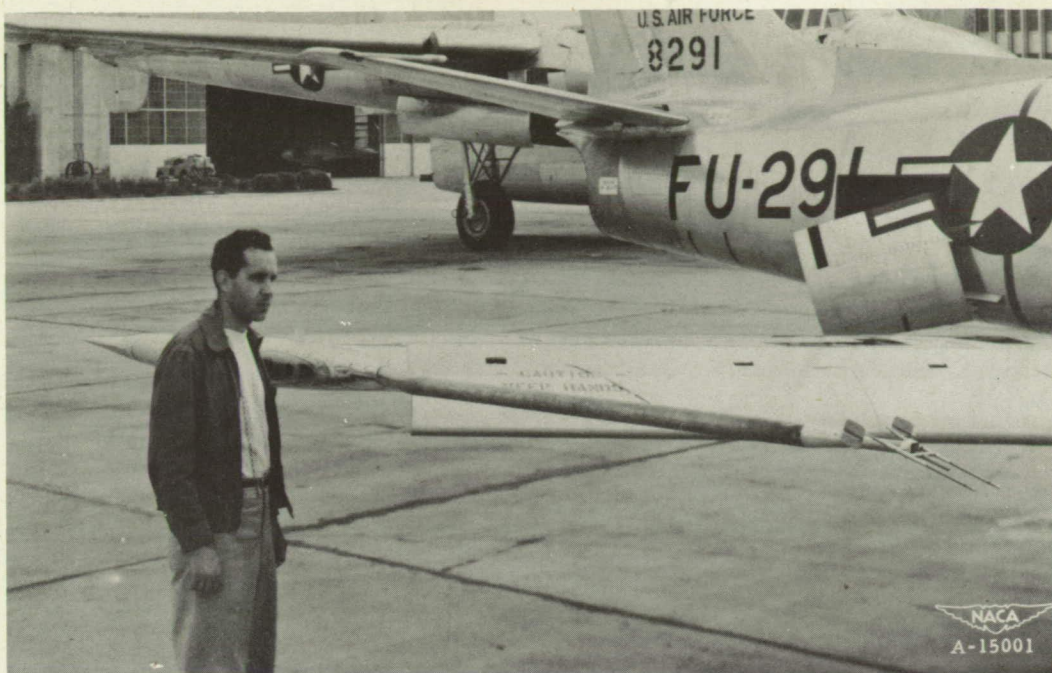
(c) Right wing boom.

(d) Left wing boom.

Figure 2.— Continued.

Page intentionally left blank
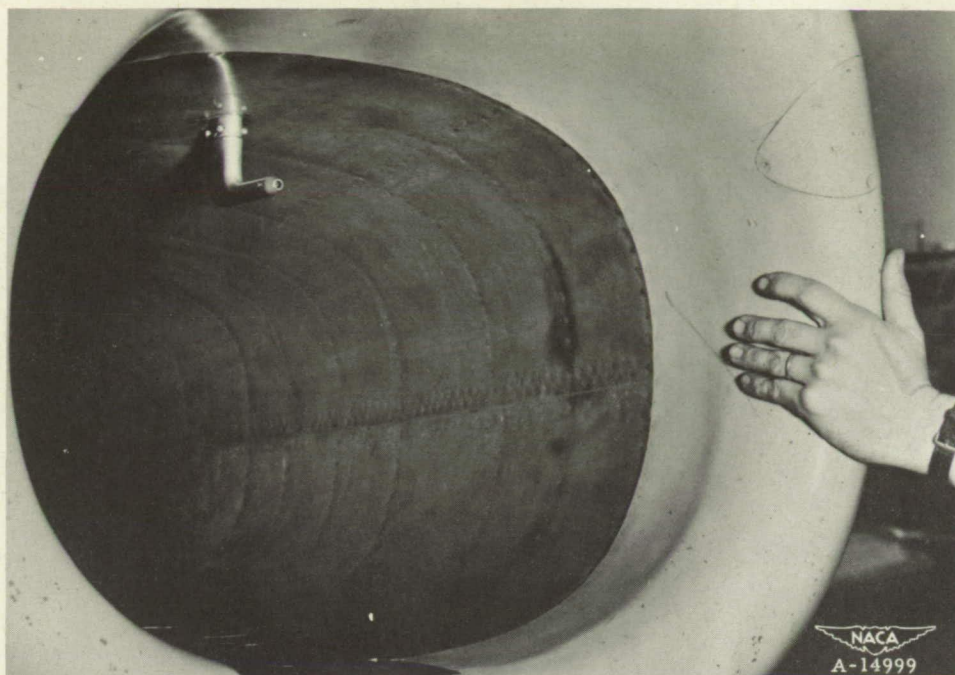
(e) Service system impact tube.

AMMUNITION
ACCESS

LOWER DOOR
FOR STEP

KEEP HOLES AND
SURFACE CLEAN
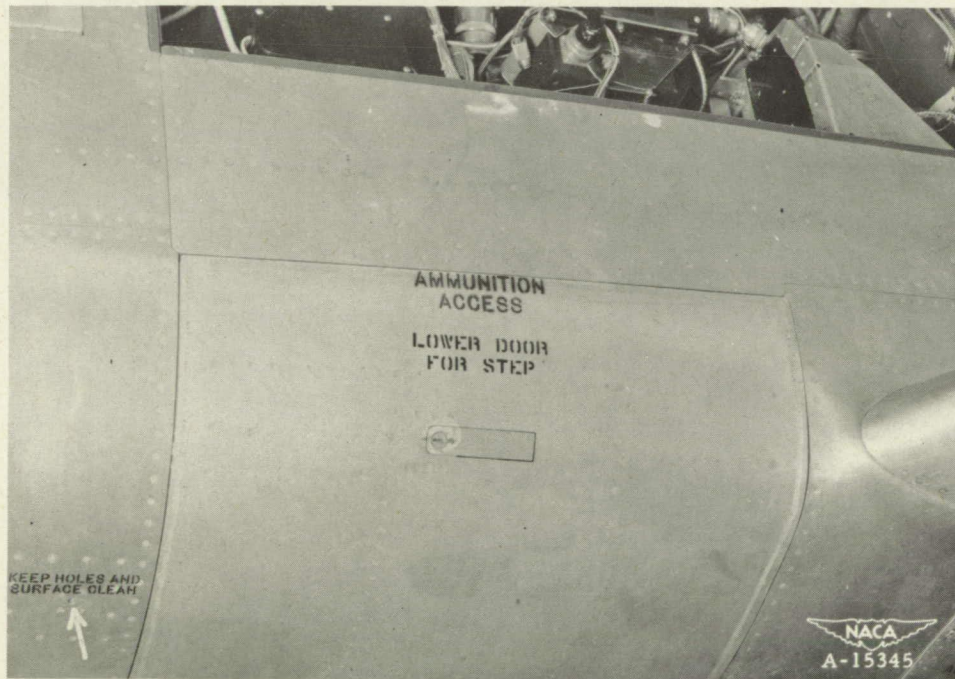
(f) Service system static orifice, lower side of
fuselage ahead of wing root.

Figure 2.— Concluded.

Page intentionally left blank

(a) Kollsman high-speed pitot-static head.
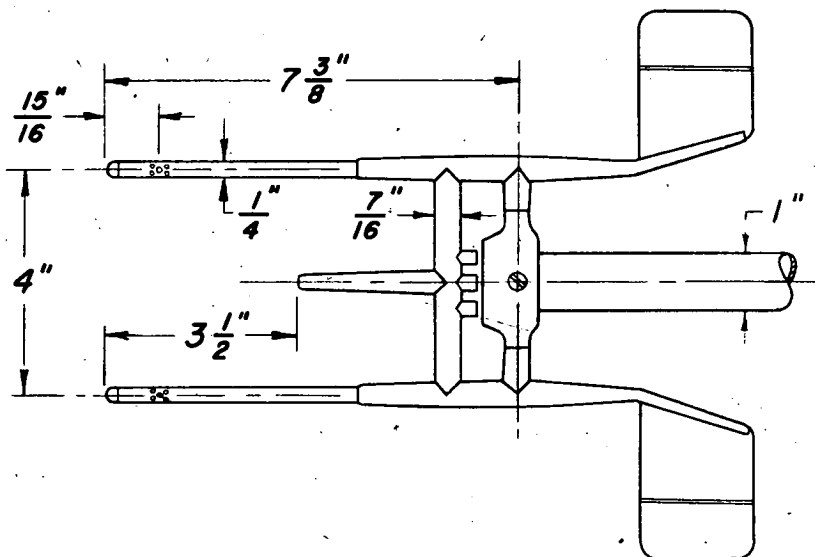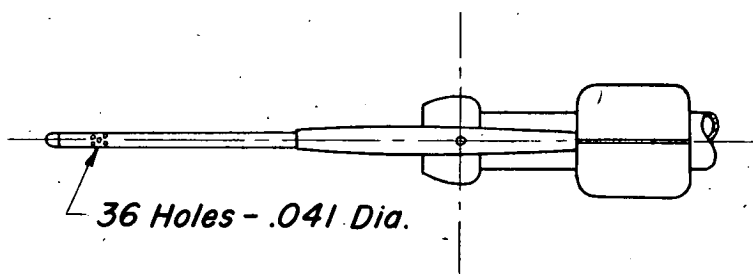
(b) NACA swiveling pitot-static head

Figure 3.- Drawings of airspeed heads used on nose and wing booms.
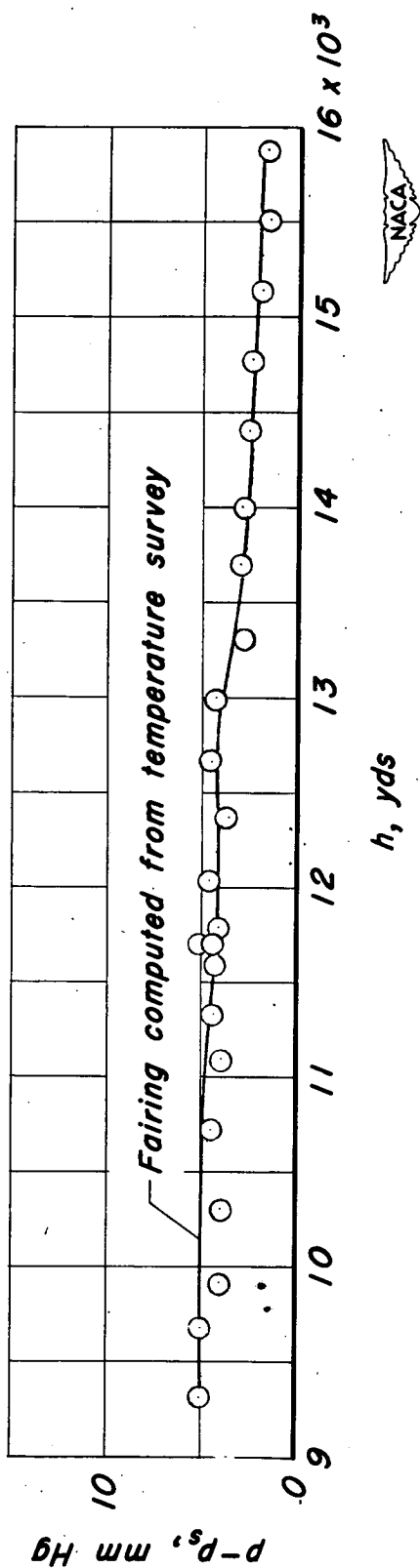
Figure 4.—Typical variation with geometric altitude of the difference between ambient pressure and NACA standard atmospheric pressure as determined from the nose-boom airspeed system during a pressure survey.
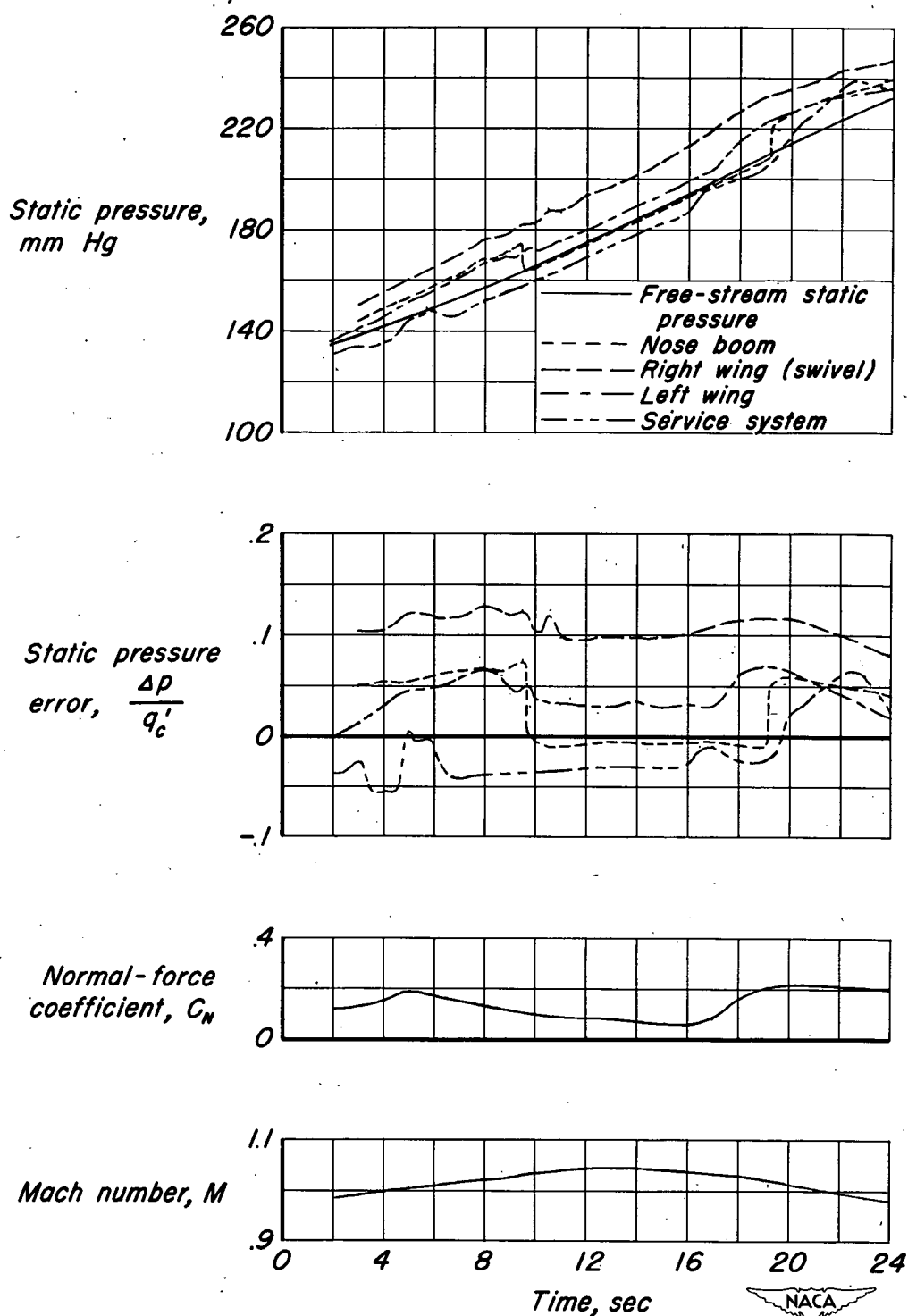
(a) High-speed run.

Figure 5.- Time history of pertinent quantities during typical airspeed calibration runs.

Static
pressure,
mm Hg

——————	Free-stream static pressure
— — —	Nose boom
— — —	Right wing (swivel)
— · —	Left wing
— — —	Service system

Static
pressure
error, $\dfrac{\Delta p}{q_c'}$

Normal-
force
coefficient,
C_N

Mach
number, M

Time, sec

NACA
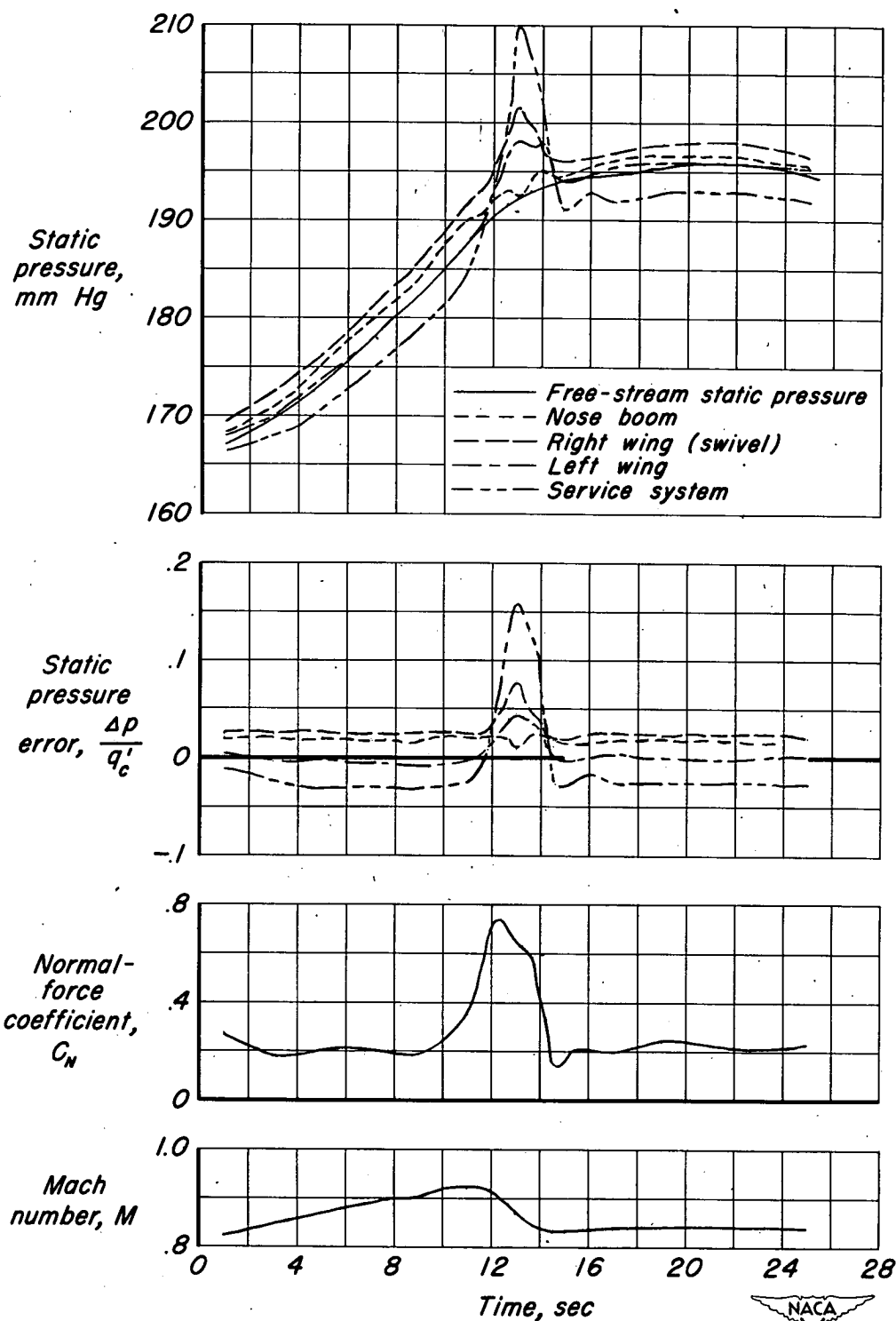
(b) Abrupt pull-up.

Figure 5. Concluded.
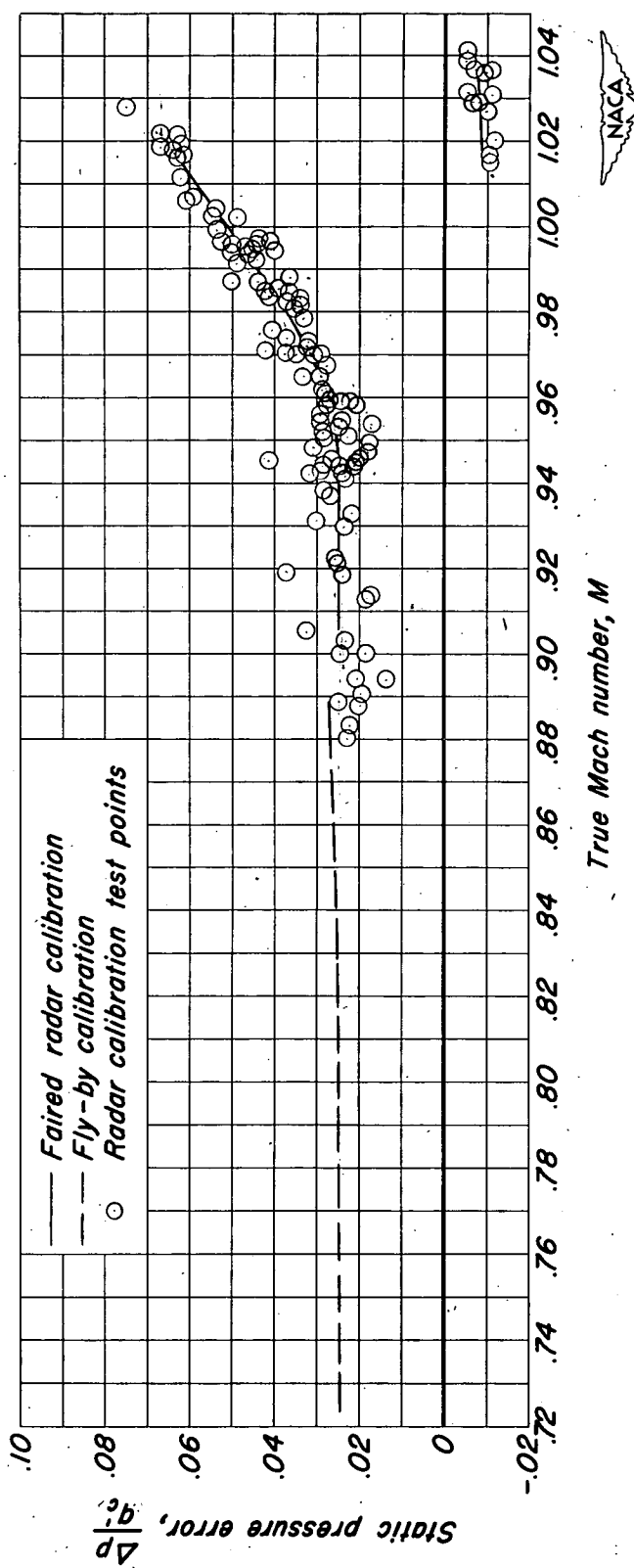
(a) Nose-boom system, C_N range 0 to 0.30.

Figure 6.— Variation with Mach number of static pressure error per unit indicated impact pressure, $\dfrac{\Delta p}{q_c'}$.

Figure 6.– Continued.

(b) Left-wing-boom system, C_N range 0 to 0.30.
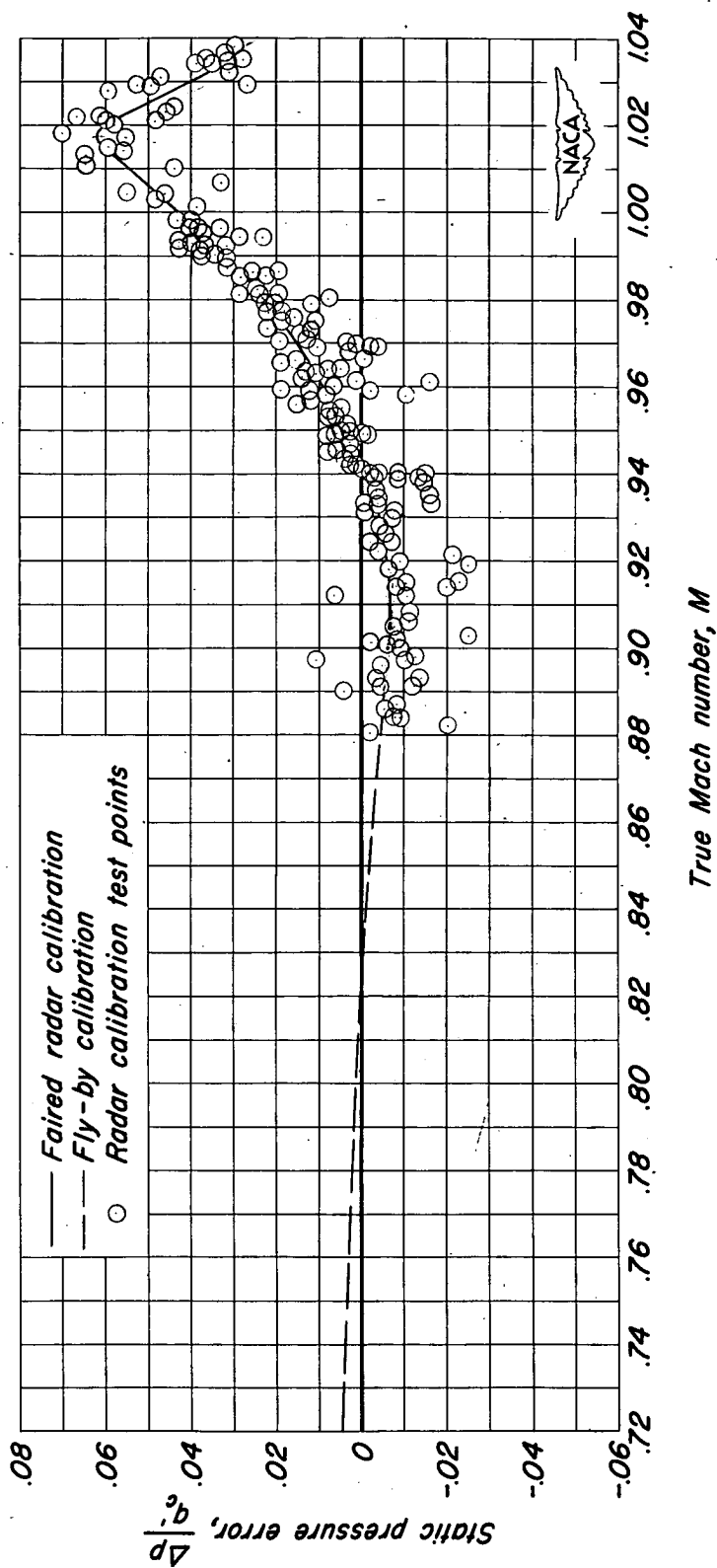
(c) Right-wing-boom system, C_N range 0 to 0.30.

Figure 6.—Continued.
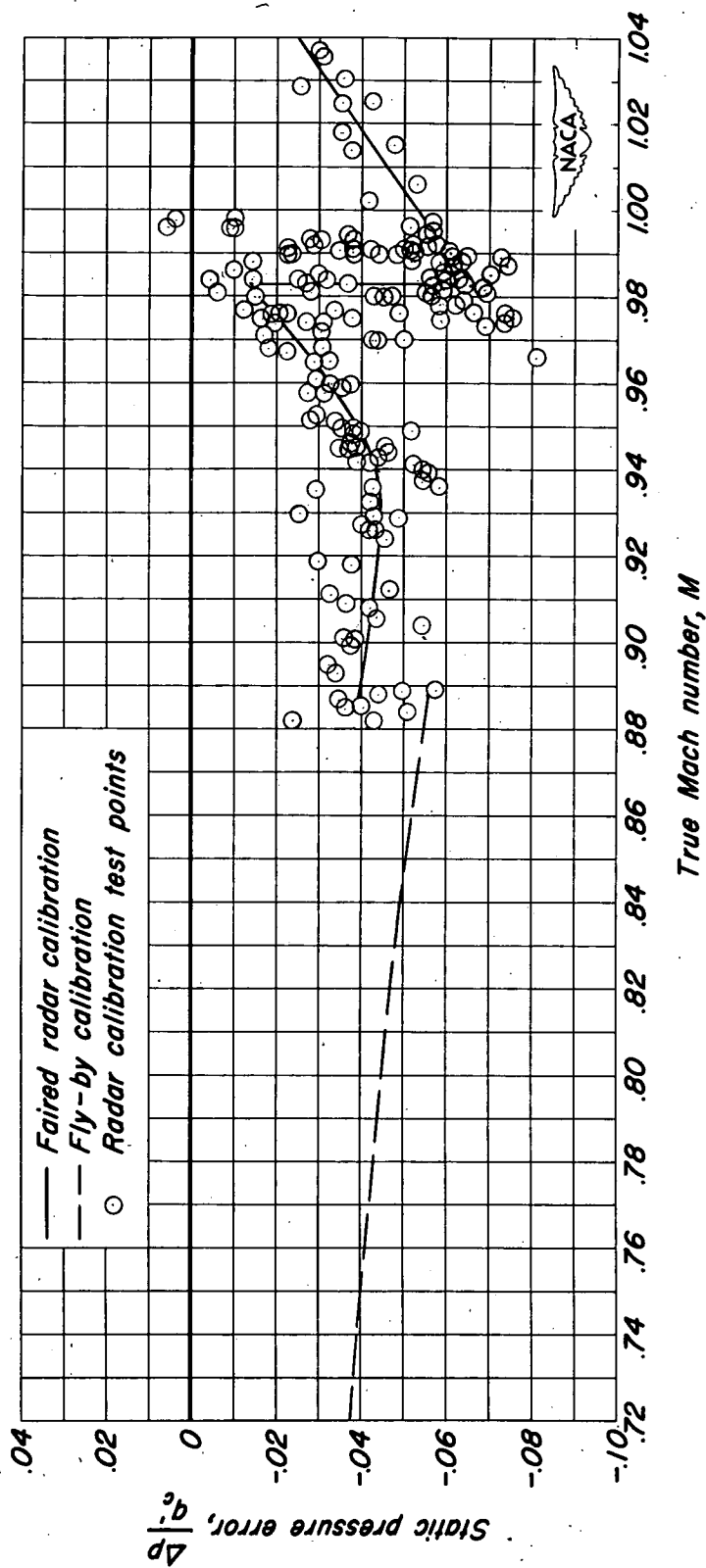
(d) Service system, C_N range 0 to 0.20.

Figure 6.— Concluded.
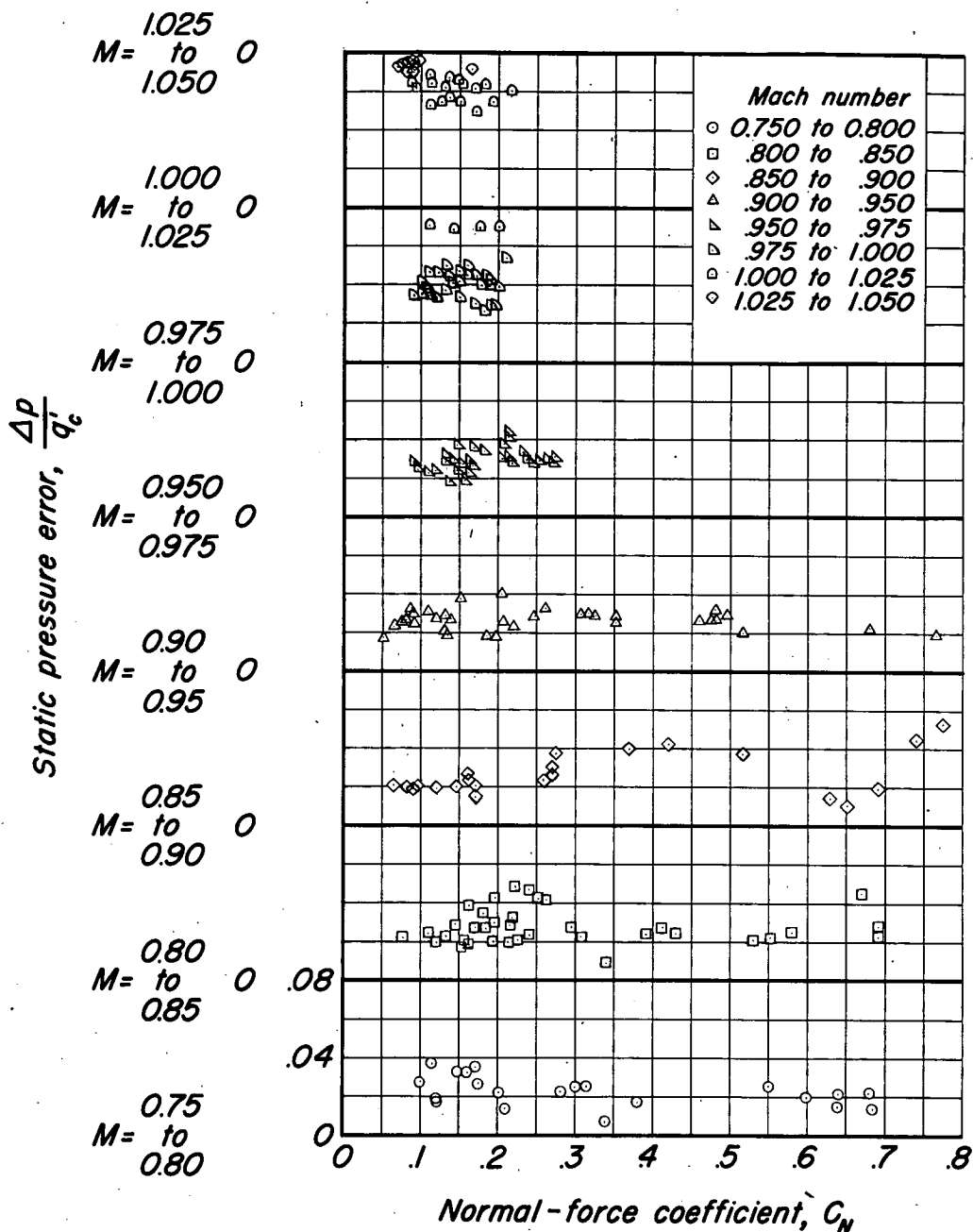
(a) Nose-boom system, M range 0.75 to 1.05.

Figure 7.- Variation with airplane normal-force coefficient, C_N, of the static pressure error per unit indicated impact pressure, $\Delta p/q_c'$, for several ranges of Mach number.
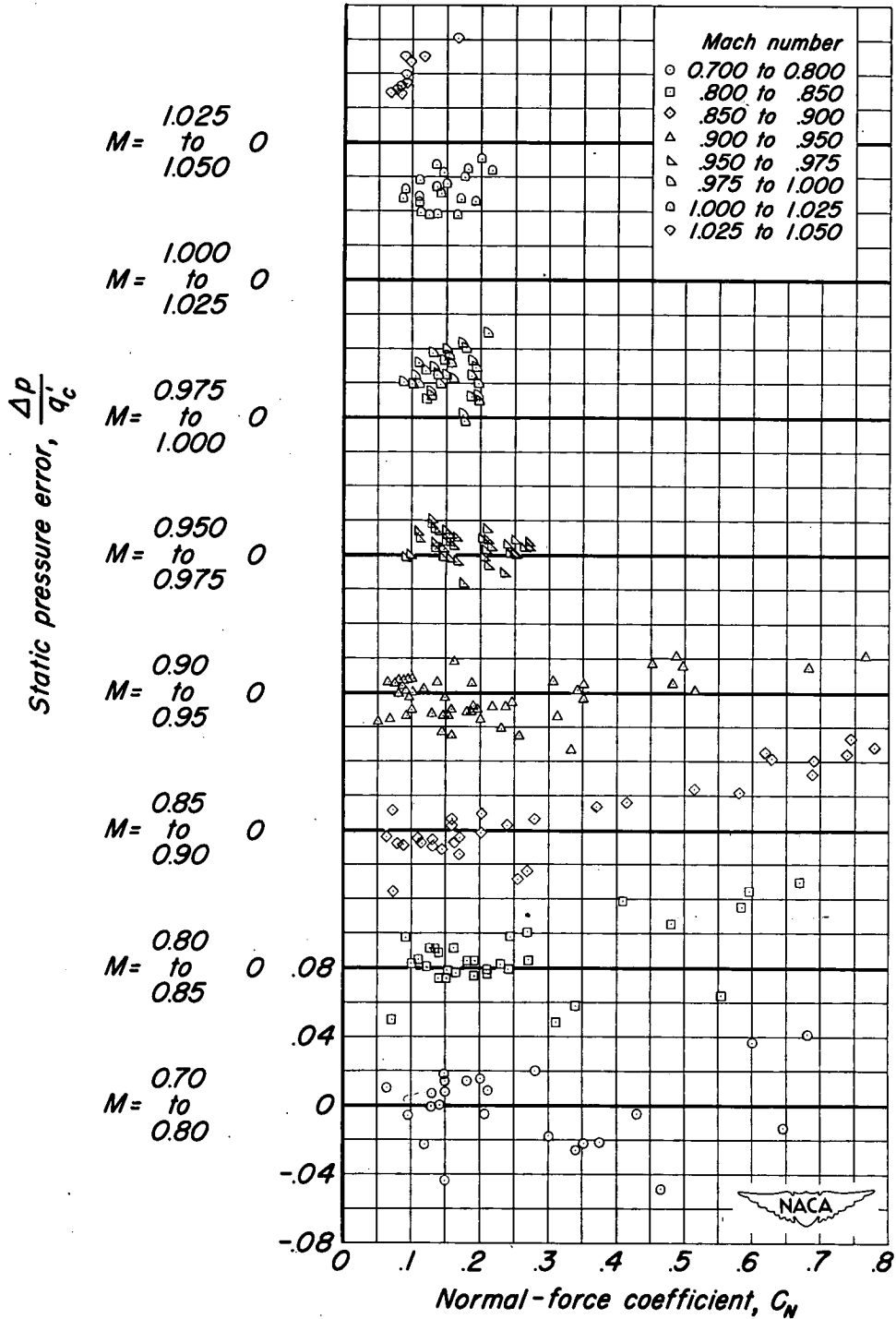
(b) Left-wing-boom system, M range 0.70 to 1.05.

Figure 7.- Continued.
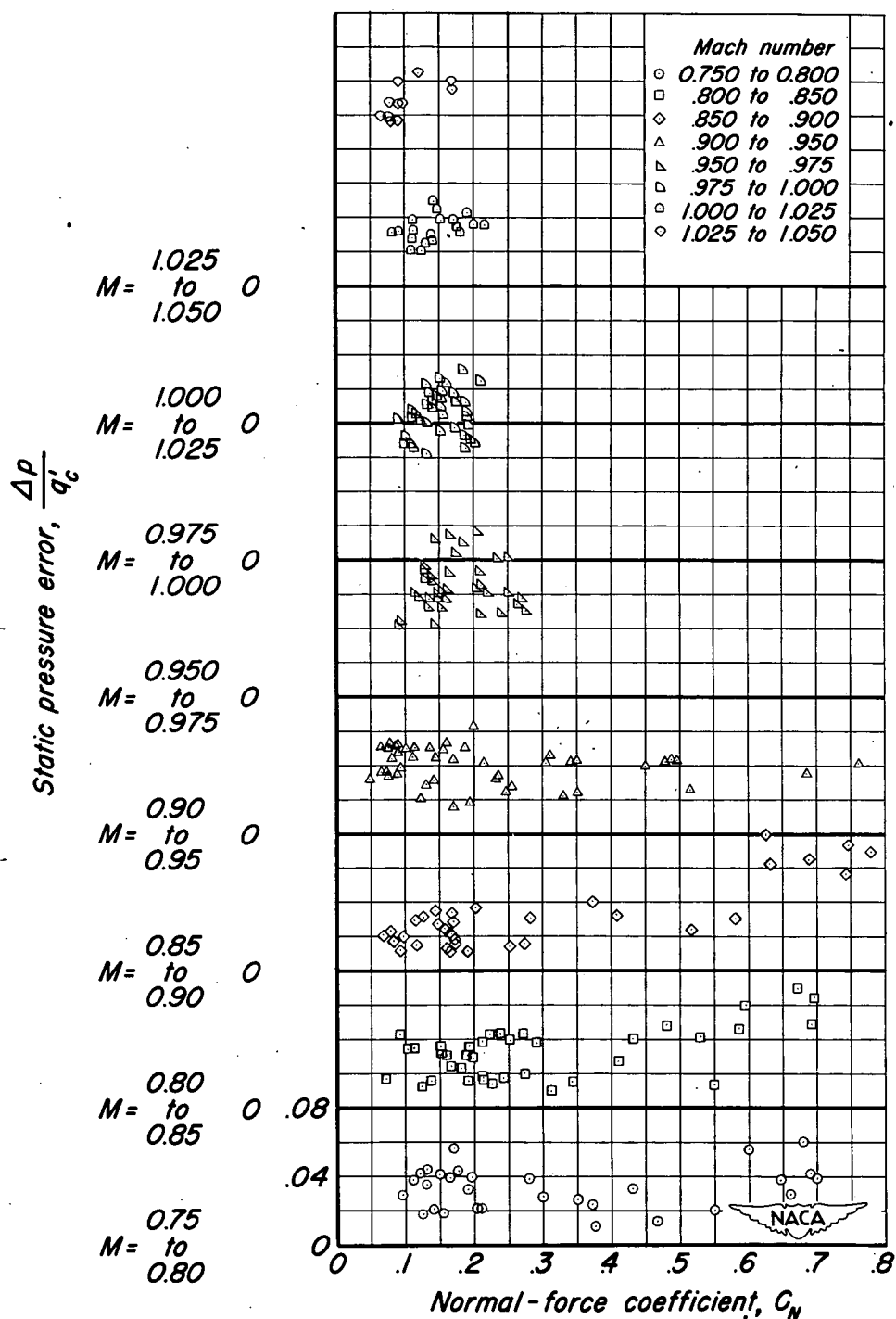
(c) Right-wing-boom system, M range
0.75 to 1.05.

Figure 7.- Continued.
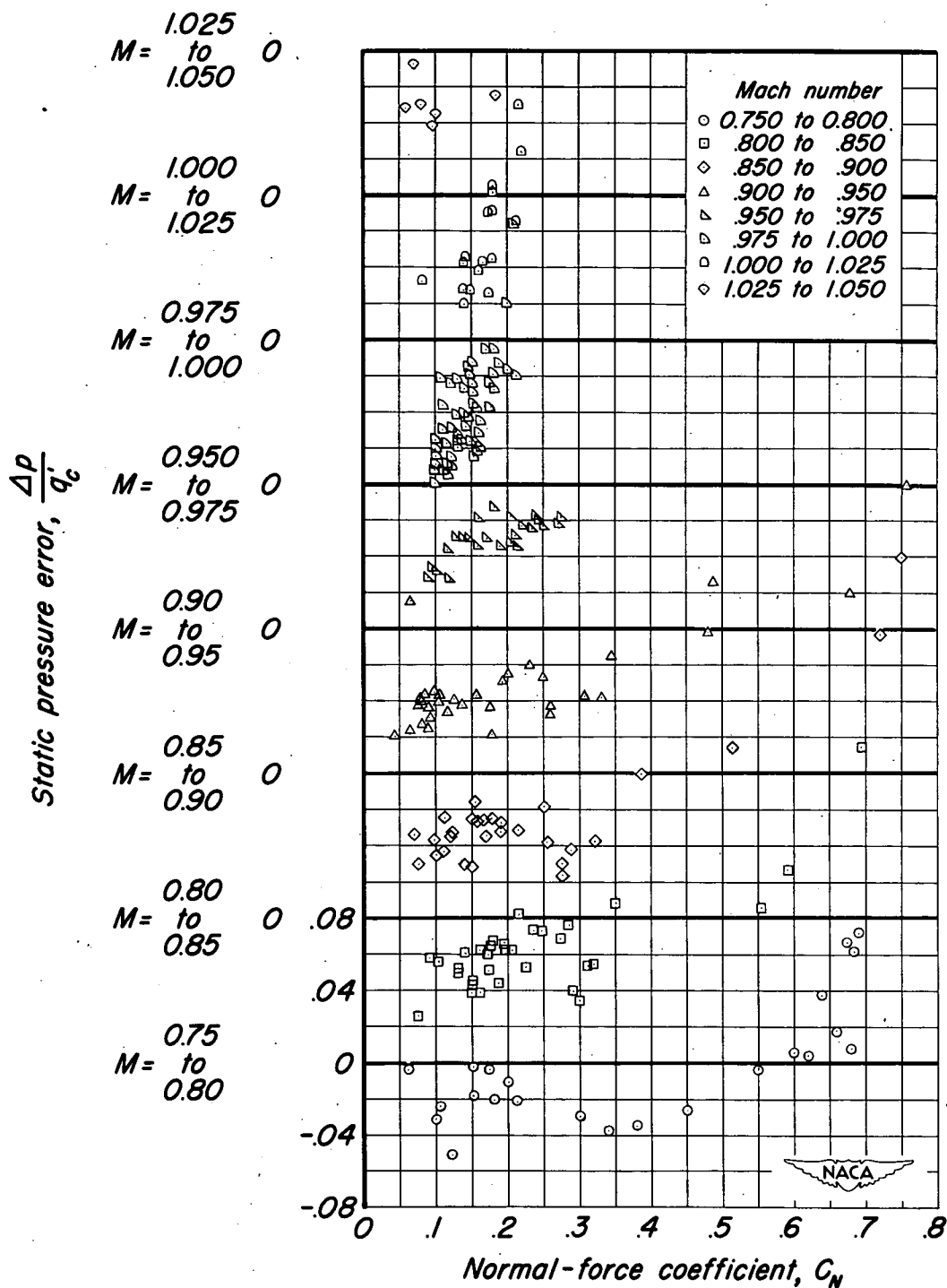
(d) Service system, M range 0.75 to 1.05.

Figure 7.- Concluded.
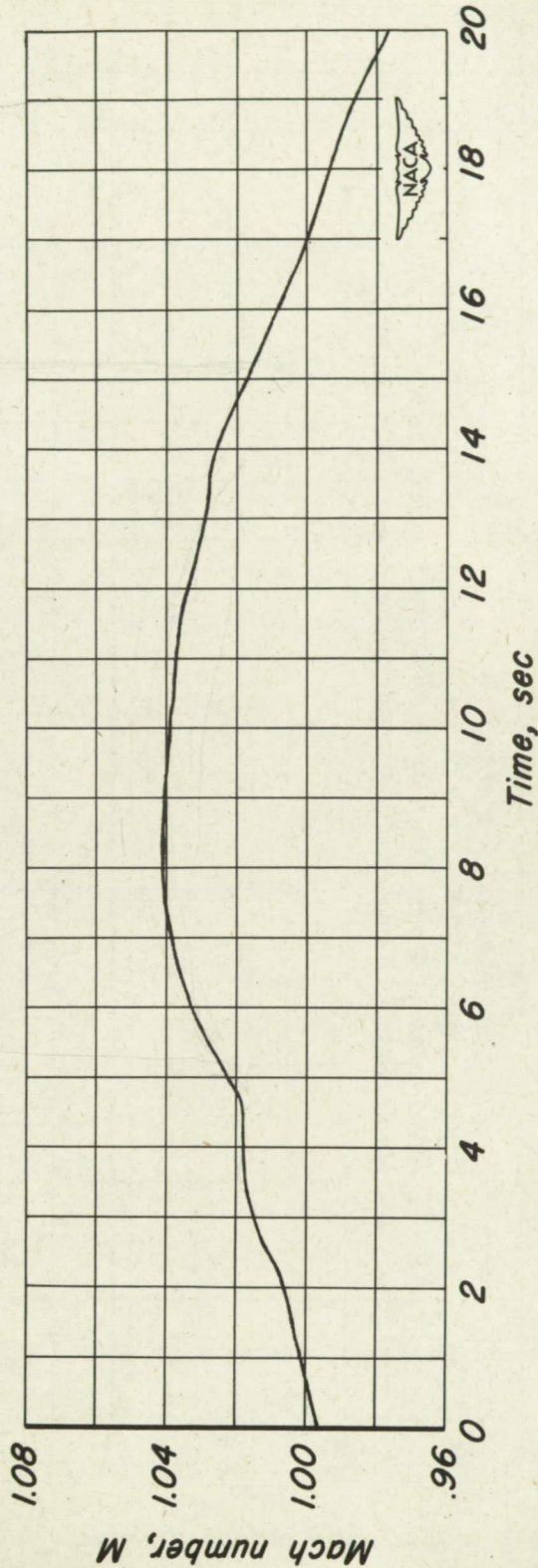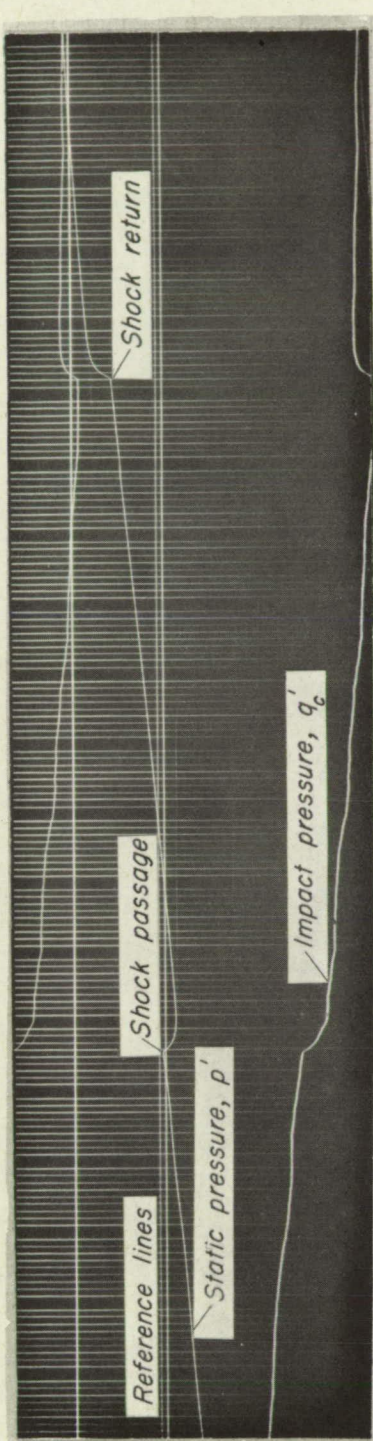
Figure 8.— Time history of high-speed dive with instrument record of indicated pressures from nose-boom airspeed system showing response to passage of fuselage-bow shock wave.
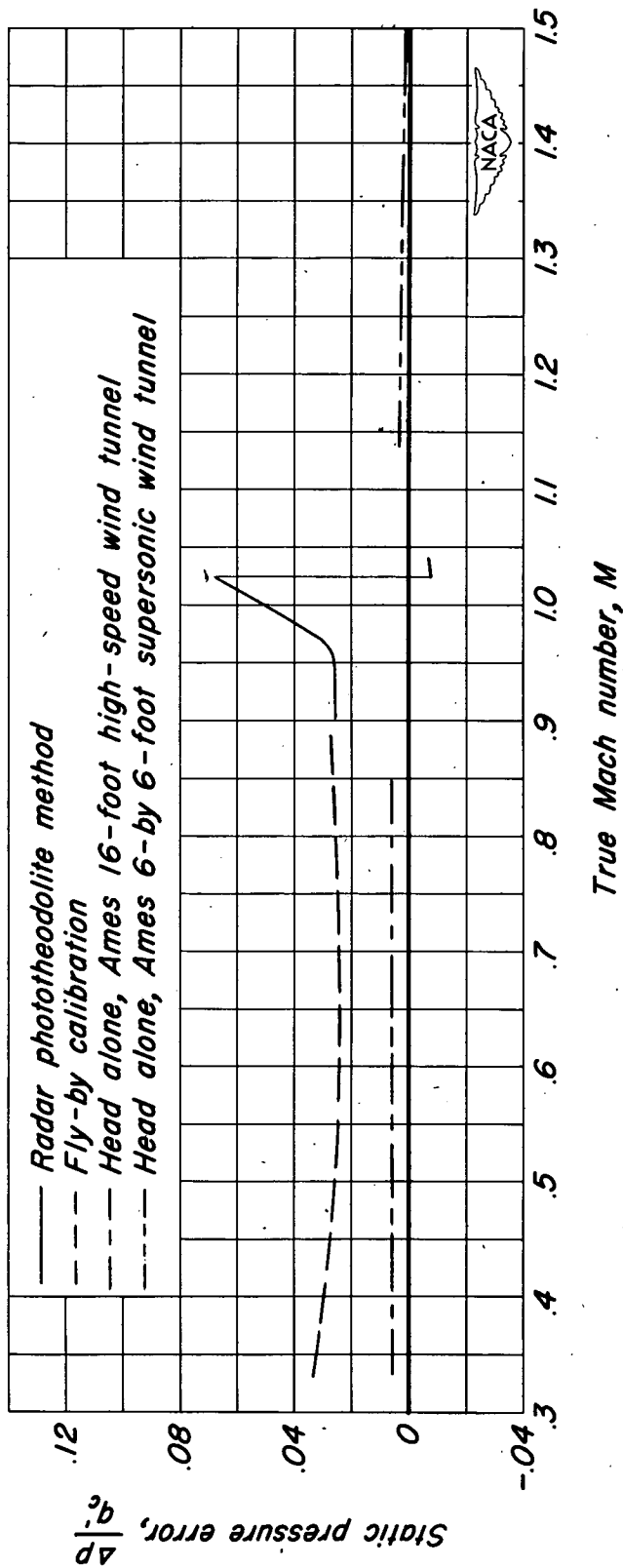
Figure 9.- Comparison of flight results for the nose-boom system with wind-tunnel results for isolated fixed airspeed head.
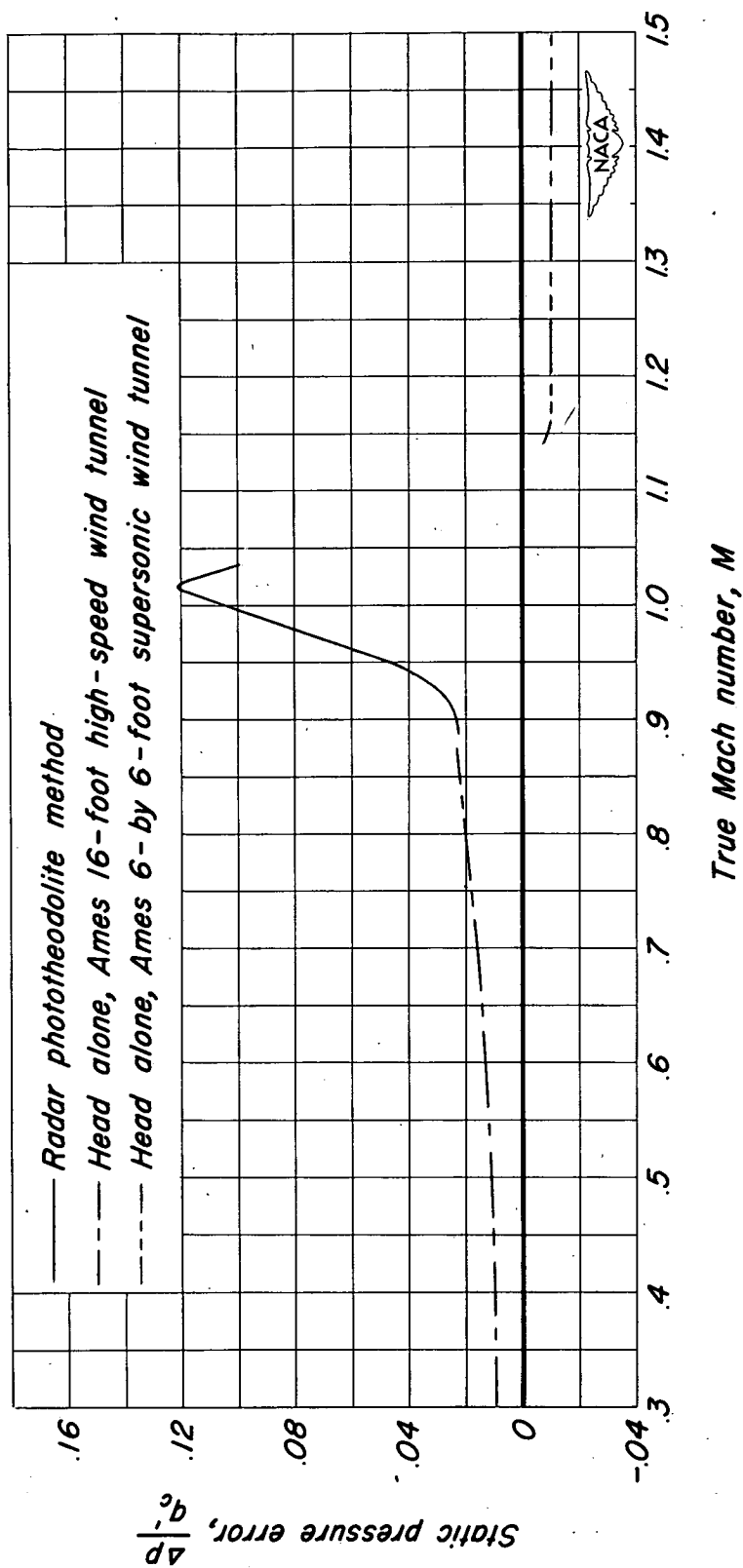
Figure 10.- Comparison of flight results for the right-wing-boom system with wind-tunnel results for isolated swiveling airspeed head.
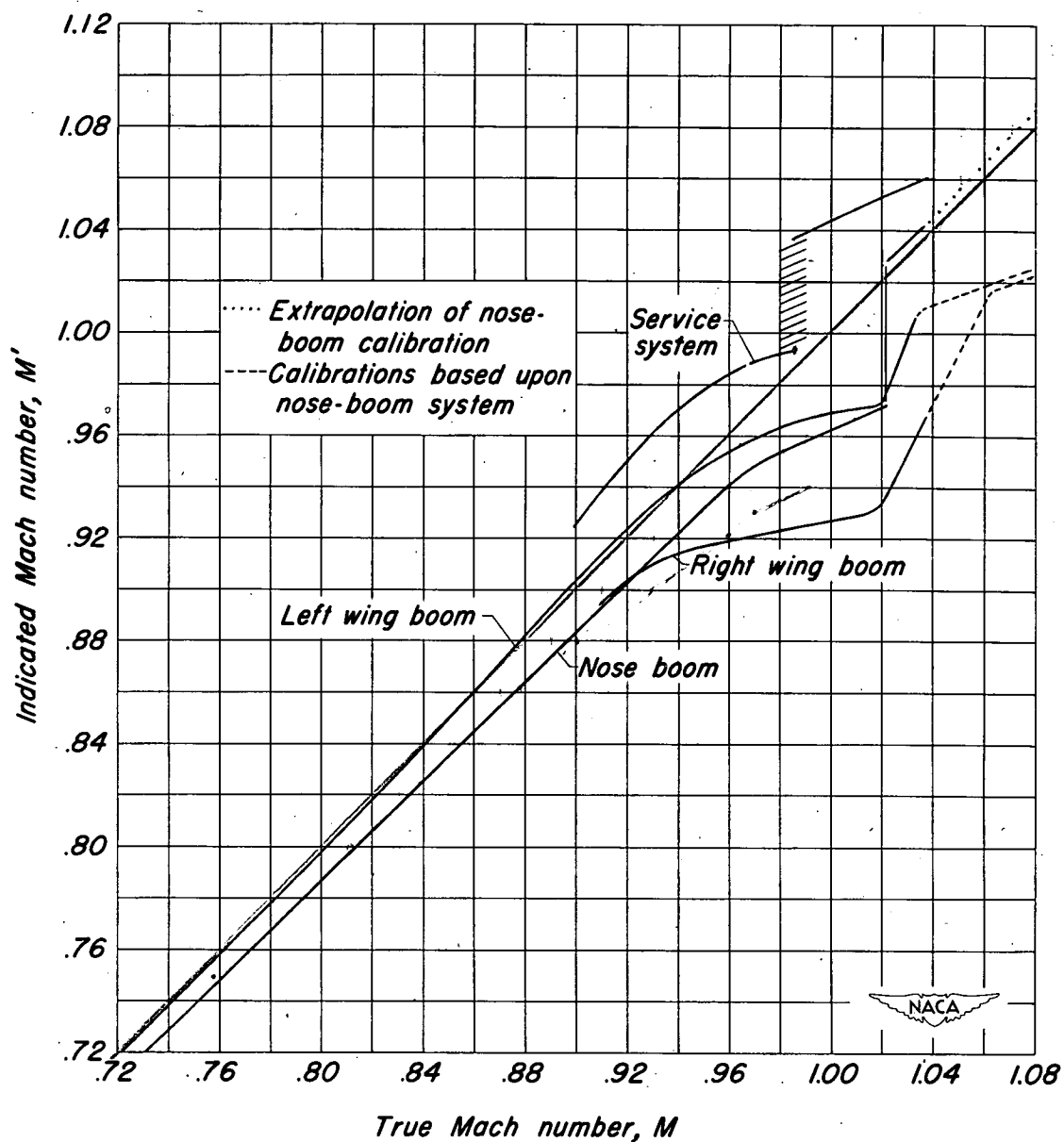
Figure 11.- Variation of indicated Mach number with true Mach number for each
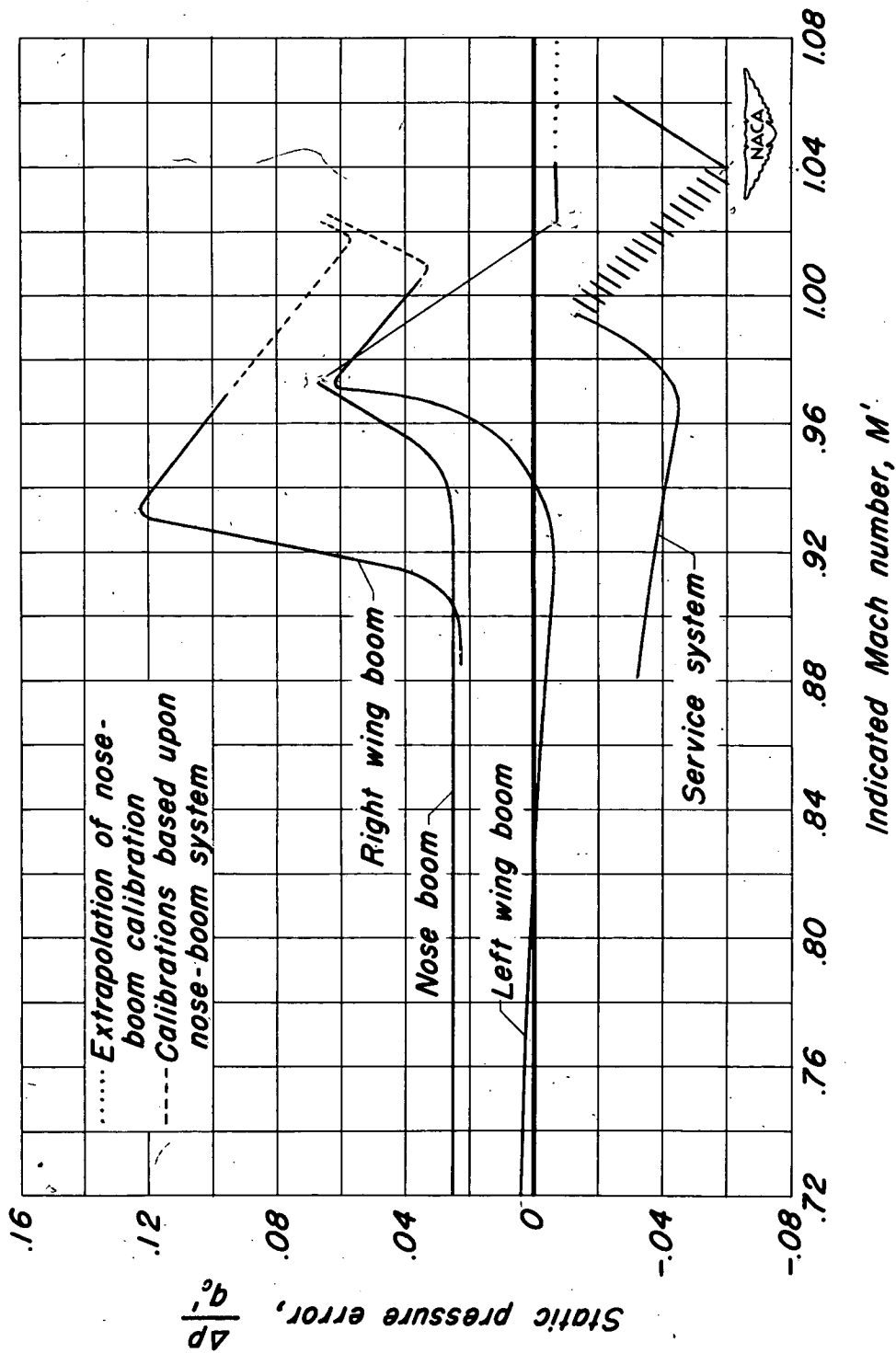   airspeed system.

Figure 12.- Variation with indicated Mach number of the static pressure error per unit indicated impact pressure for each airspeed system.